ACS APPLIED MATERIALS & INTERFACES

Research Article

www.acsami.org

Correlation between the Open-Circuit Voltage and Charge Transfer State Energy in Organic Photovoltaic Cells

Yunlong Zou and Russell J. Holmes*

Department of Chemical Engineering and Materials Science, University of Minnesota, Minneapolis, Minnesota 55455, United States

ABSTRACT: In order to further improve the performance of organic photovoltaic cells (OPVs), it is essential to better understand the factors that limit the open-circuit voltage (V_{OC}). Previous work has sought to correlate the value of V_{OC} in donor−acceptor (D−A) OPVs to the interface energy level offset (E_{DA}). In this work, measurements of electroluminescence are used to extract the charge transfer (CT) state energy for multiple small molecule D−A pairings. The CT state as measured from electroluminescence is found to show better correlation to the maximum V_{OC} than E_{DA}. The difference between E_{DA} and the CT state energy is attributed to the Coulombic binding energy of the CT state. This correlation is demonstrated explicitly by inserting an insulating spacer layer between the donor and acceptor materials, reducing the binding energy of the CT state and increasing the measured V_{OC}. These results demonstrate a direct correlation between maximum V_{OC} and CT state energy.

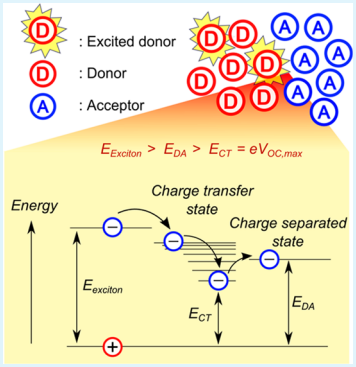

KEYWORDS: *organic photovoltaic cells, heterojunction, open-circuit voltage, charge transfer state, electroluminescence*

INTRODUCTION

Organic photovoltaic cells (OPVs) frequently adopt an electron donor−acceptor (D−A) heterojunction architecture to facilitate efficient exciton dissociation.[1,2] While driving exciton dissociation by charge transfer, the required energy offset at the D−A interface leads to an inherent energy loss during photoconversion. As a consequence, devices that adopt the D−A heterojunction architecture typically operate with lower open-circuit voltage (V_{OC}) than devices that instead rely on bulk exciton ionization, as is the case in Schottky OPVs.[3−7] In order to realize increased power conversion efficiency (η_P) in OPVs, both the short-circuit current density (J_{SC}) and V_{OC} must be optimized. Much previous work has focused on and succeeded in maximizing the device external quantum efficiency (η_{EQE}) and J_{SC}.[8−12] As such, the most significant bottleneck to further increases in efficiency is the small value of V_{OC} relative to the absorbed photon energy. It is thus critical to better understand the theoretical maximum achievable V_{OC} for a particular D−A junction and develop techniques to drive the observed V_{OC} closer to this ideal value. Previous research has demonstrated that the maximum achievable V_{OC} in a D−A heterojunction OPV can be determined at low temperature and is related to the difference between the highest occupied (HOMO) and lowest unoccupied molecular orbital (LUMO) energy levels of the donor and acceptor materials, respectively, termed the interface energy level offset (E_{DA}).[13−15] While these quantities are related, the observed maximum V_{OC} is smaller than E_{DA}, and an exact correlation requires the inclusion of an empirical energy offset term.[13] One possible source for this additional energy loss is the need to overcome the binding energy of the charge transfer (CT) state that forms after exciton dissociation.[16] The Coulombic attraction between the oppositely charged carriers serves as a barrier for further charge separation and reduces the CT state energy (E_{CT}) relative to E_{DA}. Recently, it has been demonstrated that in polymer−fullerene based OPVs a direct correlation can be made between E_{CT}, as determined by fitting the sub-bandgap feature in η_{EQE} spectra using Marcus theory, and the extrapolated V_{OC} at 0 K, termed V_0.[15,17−20] Here, we examine small molecule OPVs as model systems to establish a relationship between CT state emission energy as measured from electroluminescence and the extracted maximum achievable V_{OC} (or V_0) for multiple D−A pairings. The CT state electroluminescence energy is chosen over the fitted E_{CT} from η_{EQE} for two reasons. First, the thermalization of the CT state is a rapid process such that V_{OC} is likely impacted by the relaxed CT state.[21] The emission spectrum is likely a more direct characterization of the filled density of relaxed CT states. Second, the broad CT state absorption feature will partially overlap with fullerene absorption features for D−A pairings with a large E_{DA}. This makes it difficult to separate the measurement of E_{CT} from photocurrent generated by the fullerene in η_{EQE} spectra. In addition to correlating E_{CT} and V_0, we also demonstrate that the E_{CT} for a given D−A pairing can be tuned using dielectric spacer layers for increased V_{OC}.

EXPERIMENTAL SECTION

Organic photovoltaic cells were fabricated on prepatterned indium−tin−oxide (ITO)-coated glass substrates having a sheet resistance of ∼8−12 Ω/□. Substrates were cleaned in tergitol solution and in organic solvents and treated in UV−ozone ambient for 10 min prior to thin film deposition. All layers were deposited by high vacuum thermal

Received: April 29, 2015
Accepted: July 30, 2015
Published: August 13, 2015

DOI: 10.1021/acsami.5b03656
ACS Appl. Mater. Interfaces 2015, 7, 18306−18311

evaporation at a base pressure of $<8 \times 10^{-7}$ Torr. For all devices, a 10 nm-thick interlayer of MoO_x was deposited at 0.05 nm/s on the ITO anode.[6] In donor−acceptor bulk heterojunction (BHJ) devices, mixed organic active layers were prepared via codeposition at a total rate of 0.2 nm/s at room temperature. All OPVs were capped with a 10 nm-thick exciton blocking layer of bathocuproine (BCP).[22] Device active areas are defined by the overlap between a 100 nm-thick Al cathode layer and a prepatterned ITO anode, giving a device active area of 9 mm^2. For this study, boron subphthalocyanine chloride (SubPc ∼ 95%), chloroaluminum phthalocyanine (ClAlPc ∼ 95%), and 1,4-bis(triphenylsilyl)benzene (UGH2∼95%) were obtained from Lumtec Inc. C_{60} (∼99%) was obtained from MER Corporation, and 2-[7-(4-*N*,*N*-ditolylaminophenylen-1-yl)-2,1,3-benzothiadiazol-4-yl]methylene malononitrile (DTDCPB ∼ 97%) and 2-[7-(4-*N*,*N*-diphenylamino-phenylen-1-yl)-2,1,3-benzothiadiazol-4-yl]methylene malononitrile (DPDCPB ∼ 97%) were synthesized by Sigma-Aldrich Corp. using methods described in previous literatures.[23,24] Pentacene (∼99%) was purchased from Sigma-Aldrich Corp., and copper phthalocyanine (CuPc ∼ 95%) was purchased from Acros Organics, while BCP (∼98%) and MoO_3 (∼99.5%) were obtained from Alfa Aesar. All materials were used as received without further purification. All device parameters were measured under AM1.5G simulated solar illumination (100 mW/cm^2) using an Oriel Xe solar simulator. All variable temperature experiments were carried out in a Janis cryogenic probe station with liquid nitrogen cooling. Device temperature was monitored using a Si thermometer. Current density−voltage characteristics were measured using a Keithley 2400 source meter. Electroluminescence spectra were measured using an Ocean Optics USB4000 fiber-coupled spectrometer and a Photon Technology International QuantaMaster 4 Fluorometer.

RESULTS AND DISCUSSION

Figure 1 shows the energy landscape that excitons experience at the D−A interface prior to dissociation into separated charge carriers. The first step is charge transfer, during which the electron (hole) is transferred to the acceptor (donor), sacrificing part of the original exciton energy. The partially separated exciton now forms an intermediate state, namely, the CT state. The CT state experiences rapid thermalization, leading to an additional loss of energy. The relaxed CT state is Coulombically bound, frustrating further separation.[25] Within the entire photoconversion process, the CT state is the lowest energy state and thus should determine the theoretical maximum achievable V_{OC} of the OPV.

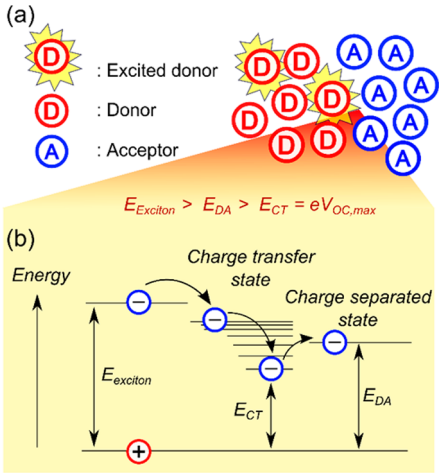

Figure 1. (a) Conversion of an exciton into separated charge carriers at an electron donor−acceptor (D−A) interface. (b) Energy landscape for the process depicted in (a). Electrons (holes) will transfer to the acceptor (donor) and form a CT state. The CT state is Coulombically bound after rapid thermalization, frustrating further separation. Ideally, the exciton energy ($E_{Exciton}$) is larger than the D−A interface energy level offset (E_{DA}). The CT state energy (E_{CT}) is the smallest among those involved in photogeneration and is equal to the maximum achievable V_{OC} multiplied by elemental charge.

Experimentally, the theoretical maximum achievable V_{OC} is typically estimated from the temperature dependence of V_{OC}, which can be described by rearranging the Shockley equation under open-circuit conditions as[13,26]

$$eV_{OC} \approx E_{eff} - nk_BT \ln\left(\frac{J_0}{J_{ph}(V_{OC})}\right) \quad (1)$$

where E_{eff} is the effective energy gap and also the limit for maximum V_{OC}, n is the ideality factor, k_B is the Boltzmann constant, e is the elementary charge, J_0 is a temperature independent prefactor, and $J_{ph}(V_{OC})$ is the photocurrent under open-circuit conditions. The energy E_{eff} is directly related to the lowest-energy intermediate state in the exciton dissociation process. In the case of a D−A heterojunction, E_{eff} equals the CT state energy.[15] In reality, the V_{OC} is also limited by the quasi-Fermi level offset at finite illumination intensity, and the observed V_{OC} will often deviate from the dependence of eq 1 and plateau at low temperature.[13,26,27] Thus, the extrapolated V_{OC} at 0 K, i.e., V_0, is often chosen to approximate the theoretical maximum achievable V_{OC} and E_{eff}.[15,26,28]

The temperature dependence of V_{OC} was measured for BHJ OPVs having the structure ITO/MoO_x 10 nm/mixed active layer 60 nm/BCP 10 nm/Al 100 nm, using a variety of different donor materials including SubPc, DPDCPB, DTDCPB, ClAlPc, and CuPc. All devices are fabricated with an acceptor material of C_{60}. The inclusion of an interlayer of MoO_x ensures that the V_{OC} is not limited by the energy levels of the electrodes.[6,23,24,29] A uniformly mixed active layer with a D:A volume ratio of 1:1 is chosen to maximize the D−A interface area and minimize the impact of exciton bulk-ionization as described in previous literature.[7,30] All devices exhibit a monotonic decrease in V_{OC} with increasing temperature, as shown in Figure 2a. The temperature dependence of V_{OC} for the D−A pairing of pentacene-C_{60} is replotted from ref 13.[13] The value of V_0 for each D−A pairing is obtained by linearly extrapolating the temperature dependence of V_{OC} to 0 K based on data in the temperature range of 210−300 K for the D−A pairing of DPDCPB-C_{60} and 190−300 K for all other D−A pairings. The error bars are taken as the sum of the 95% confidence interval and the experimentally measured standard deviation of V_{OC}. Literature values of the energy levels for materials used in this study are listed in Table 1 for the calculation of E_{DA}. The literature values for the various HOMO energy levels are determined via photoelectron emission spectroscopy, and the literature values for the various LUMO energy levels are determined via soft X-ray spectroscopy, inverse photoelectron emission spectroscopy, or cyclic voltammetry.[24,31,32]

A comparison between V_0 and E_{DA} for each D−A pairing is shown in Figure 2b, and a linear relationship is found between the two parameters. However, similar to previous studies, the observed linear relationship does not pass through the origin (the intercept is ∼0.38 eV).[13,26] This lack of agreement highlights the fact that E_{DA} does not simply equal E_{CT}, due chiefly to the binding energy of the CT state. In order to better correlate the theoretical maximum achievable V_{OC} and D−A interface energetics, a direct measurement of E_{CT} is necessary. Here, we use CT state electroluminescence spectroscopy to

DOI: 10.1021/acsami.5b03656
ACS Appl. Mater. Interfaces 2015, 7, 18306−18311

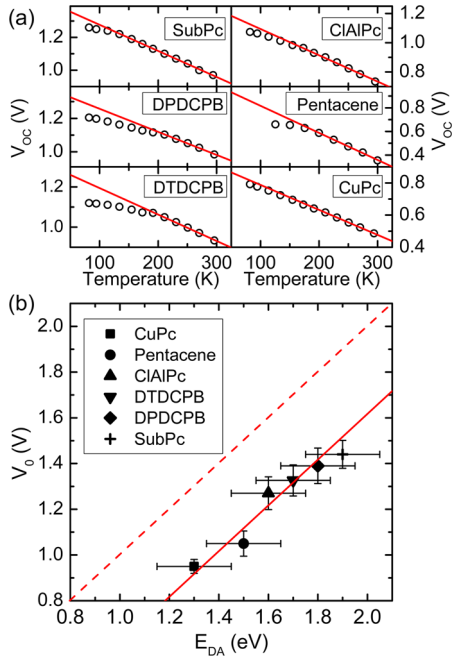

Figure 2. (a) Temperature dependence of V_{OC} for BHJs (D:A ratio = 1:1) based on different donor materials and C_{60}. The temperature dependence of V_{OC} for the D−A pairing of pentacene-C_{60} is replotted from ref 13. The linear extrapolations of V_{OC} to 0 K are based on data in the temperature range of 210−300 K for the D−A pairing of DPDCPB-C_{60} and 190−300 K for all other D−A pairings. (b) The correlation between the linearly extrapolated V_{OC} at 0 K (V_0) and E_{DA}. The solid line is fit to the data with a slope of unity, and the dashed line represents perfect positive correlation. The vertical error bars are taken as the sum of the 95% confidence interval and the experimentally measured standard deviation of V_{OC}.

Table 1. Energy Levels of Materials Studied

material[a]	HOMO (eV)	LUMO (eV)	E_{DA}[b] (eV)	ref
SubPc	5.6	3.2	1.9	31
DPDCPB	5.5	3.4	1.8	24
DTDCPB	5.4	3.4	1.7	24
ClAlPc	5.3	3.4	1.6	31
pentacene	5.2	3	1.5	32
CuPc	5.0	3.3	1.3	31, 42
C_{60}	6.2	3.7	-	32

[a]SubPc, boron subphthalocyanine chloride; DPDCPB, 2-[7-(4-*N*,*N*-diphenylaminophenylen-1-yl)-2,1,3-benzothiadiazol-4-yl]methylene malononitrile; DTDCPB, 2-[7-(4-N,N-ditolylaminophenylen-1-yl)-2,1,3-benzothiadiazol-4-yl]methylene malononitrile; ClAlPc, chloroaluminum phthalocyanine; CuPc, copper phthalocyanine. [b]Energy level offset between the HOMO level of donor material and the LUMO level of C_{60}.

determine E_{CT}.[33−36] Under electrical excitation, CT states are formed across the D−A interface and may recombine radiatively. In most cases, for current injection levels (~80 mA/cm^2) slightly higher than J_{SC}, only CT state electroluminescence is observed, avoiding direct exciton decay on either the donor or the acceptor material. The observed CT state electroluminescence spectra are broad and located in the near-infrared region of the spectrum with a typical full-width at half-maximum (fwhm) of 0.2−0.3 eV, as shown in Figure 3a. Electroluminescence spectra are fit using a single Gaussian function, with the peak position taken as the value of E_{CT} and

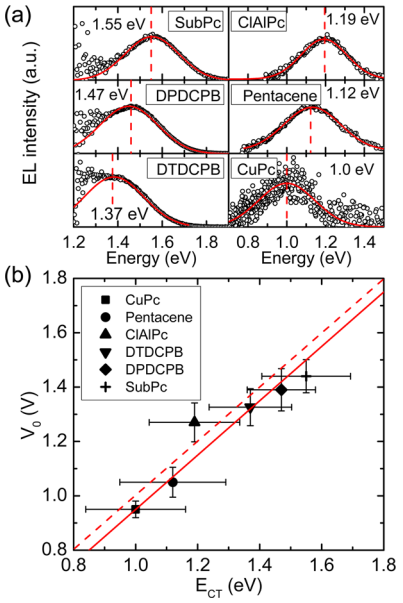

Figure 3. (a) Electroluminescence (EL) spectra for BHJs based on six different donor materials paired with an acceptor layer of C_{60} measured under a current density of ~80 mA/cm^2. Each spectrum is fit with a single Gaussian function, with the peak energy taken as the charge-transfer state energy (E_{CT}). (b) The correlation between the linearly extracted maximum achievable V_{OC}, (i.e. V_0), and E_{CT}. The solid line is fit to the data with a slope of unity, and the dashed line represents perfect positive correlation. The horizontal error bars are determined from the full-width at half-maximum of the CT state emission feature.

the fwhm taken as the error bar. A comparison between the extrapolated V_0 and E_{CT} for each D−A pairing is plotted in Figure 3b. The solid line is a linear fit to the data with a slope of unity while the dashed line represents perfect positive correlation. A clear linear relationship is preserved. More importantly, the linear relationship between E_{CT} and V_0 has almost zero intercept (~0.05 eV), confirming that a stronger correlation can be made between E_{CT} and V_0, over E_{DA} and V_0. Further theoretical analysis on accurately extracting E_{CT} from the CT state electroluminescence may help eliminate the small intercept observed in our fitting results.

In comparing the measured values for E_{DA} and E_{CT}, a fairly constant offset of ~0.33 eV is observed. In previous work, this energy shift has been ascribed to the binding energy of the CT state.[37] As a result, the V_{OC} can be improved if the binding energy of the CT state is reduced. Previously, Campbell et al. have demonstrated that the exciton dissociation and CT recombination rates in a tetracene-C_{60} planar heterojunction (PHJ) could be tuned by inserting a wide-energy-gap spacer layer between the donor and acceptor.[38] Both the J_{SC} and η_P are enhanced with the incorporation of a 1 nm-thick spacer layer. Liu et al. have carried out a theoretical analysis for this device architecture to model the dependence of V_{OC} on the spacer layer thickness. The model calculates V_{OC} from the CT state density at the D−A interface and predicts that the V_{OC} will follow the trend of J_{SC}.[39]

Here, we instead focus on how the presence of a spacer layer impacts the initial size of the CT state and, hence, V_{OC}. A thin spacer layer of UGH2 is inserted at the D−A interface in PHJ OPVs. UGH2 is a wide energy gap host material used in the construction of blue organic light-emitting devices and is characterized by a deep HOMO level (7.2 eV) and a shallow

DOI: 10.1021/acsami.5b03656
ACS Appl. Mater. Interfaces 2015, 7, 18306−18311

LUMO level (2.8 eV).[40] Insertion of the UGH2 layer permits spatial separation between holes residing in the HOMO level of the donor material and electrons residing in the LUMO level of the acceptor material.

Planar devices based on donor layers of CuPc and ClAlPc were constructed with a spacer layer of UGH2 included at the D−A interface in order to vary the initial separation of the CT state. Here, the spacer layer is found to have a deleterious effect on the J_{SC} for both devices as shown in Figure 4a. The

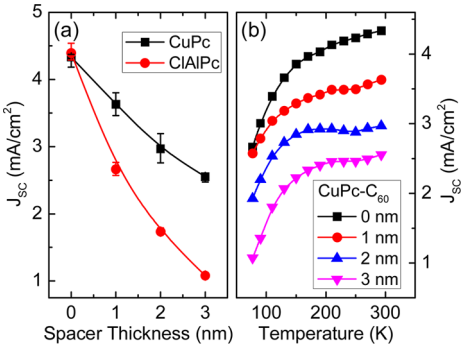

Figure 4. (a) Measured values of J_{SC} for planar heterojunction OPVs (ITO/CuPc 20 nm or ClAlPc 15 nm/UGH2 x nm/C_{60} 40 nm/BCP 10 nm/Al 100 nm) as a function of UGH2 spacer layer thickness. (b) Temperature dependence of J_{SC} for the CuPc-C_{60} device of (a) as a function of UGH2 spacer layer thickness.

incorporation of a spacer layer is also found to impact the temperature dependence of J_{SC}. Previous literatures have observed a decrease in J_{SC} with decreasing temperature.[6,13] Interestingly, the temperature dependence of J_{SC} changes as the thickness of the spacer layer increases, as depicted in Figure 4b. The J_{SC} shows a plateau when cooling from 250 to 190 K in devices containing a spacer layer of UGH2 for the D−A pairing of CuPc-C_{60}. The plateau in J_{SC} may reflect a counterbalance between increasing exciton lifetime and decreasing CT state dissociation yield at low temperature.[2,38]

The V_{OC} is found to increase monotonically as the thickness of the UGH2 layer increases (Figure 5a). This is in contrast to the dependence of V_{OC} on the spacer layer thickness predicted by Liu et al.,[39] which is calculated based on CT state density obtained from a numerical device model and will thus follow the trend of J_{SC}. Our experimental result indicates that the spacer layer impacts not only the CT state density but also the CT state energy. As a result, even with a 3 nm-thick spacer layer, no reduction in V_{OC} is observed.

The CT state energy is ultimately the electric potential difference between the HOMO level of the donor material and the LUMO level of the acceptor material (E_{DA}) less the CT state binding energy. In the simplest incarnation, the CT state binding energy is the Coulombic attraction between oppositely charged carriers. This permits the relationship between E_{CT} and the spacer layer thickness to be written using a simple Coulombic attraction as

$$E_{CT} = E_{DA} - E_b \frac{a_0}{a_0 + \frac{\varepsilon_{spacer}}{\varepsilon_{active}} d} \qquad E_b = \frac{e^2}{4\pi\varepsilon_0 \varepsilon_{active} a_0} \tag{2}$$

where E_b and a_0 are the binding energy and initial separation of the CT state in the absence of a spacer layer, d is the thickness of the spacer layer, ε_0 is the permittivity of vacuum, ε_{active} is the relative permittivity of the active material, and ε_{spacer} is the

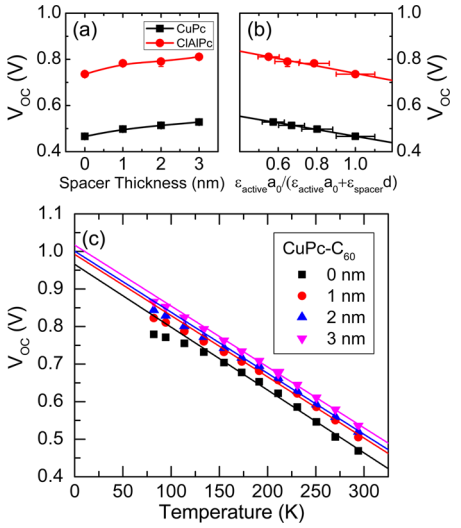

Figure 5. (a) Measured values of V_{OC} for planar heterojunction OPVs (ITO/CuPc 20 nm or ClAlPc 15 nm/UGH2 x nm/C_{60} 40 nm/BCP 10 nm/Al 100 nm) as a function of UGH2 spacer layer thickness. (b) Modeling the increase of E_{CT} with the incorporation of a spacer layer by fitting the spacer thickness dependence of V_{OC}. (c) Temperature dependence of V_{OC} for the D−A pairing of CuPc-C_{60} with the device architecture in (a) as a function of UGH2 spacer layer thickness. The linear extrapolations of V_{OC} to 0 K are based on data in the temperature range of 150−300 K.

relative permittivity of the spacer layer. Previously in Figure 3b, we have established the correlation between E_{CT} and the theoretical maximum achievable V_{OC}. Therefore, by replacing E_{eff} with the expression of E_{CT}, eq 1 can be rewritten as

$$eV_{OC} = E_{DA} - nkT \ln\left(\frac{J_0}{J_{ph}(V_{OC})}\right) - E_b \frac{a_0}{a_0 + \frac{\varepsilon_{spacer}}{\varepsilon_{active}} d} \tag{3}$$

Equation 3 permits a direct correlation to be made between V_{OC} and the spacer layer thickness (d), allowing the parameter a_0 to be extracted by linearly fitting the data in Figure 5b. In order to reduce the number of fitting parameters, values of ε_{spacer} and ε_{active} are estimated using the near-infrared refractive indices of UGH2 (ε_{spacer} = 2.5) and the active material mixture (D:A mixing ratio = 1:1). The CT state binding energy, E_b, is written as a function of a_0 and ε_{active} using eq 2, meaning the slope of the linear fit in Figure 5b is now only a function of a_0. For the D−A pairing of CuPc-C_{60}, a fit value of a_0 = (2.6 ± 0.3) nm is obtained with ε_{active} = 3.8, corresponding to E_b = (0.15 ± 0.02) eV. For the D−A pairing of ClAlPc-C_{60}, a fit value of a_0 = (1.7 ± 0.7) nm is obtained with ε_{active} = 5.4, corresponding to E_b = (0.16 ± 0.07) eV. Error bars are determined form the 95% confidence interval of the fit. The extracted values of a_0 suggest that in the absence of a spacer layer, the CT state is tightly bound, likely spanning two molecules.

Aside from a reduction in V_{OC}, a reduction in the forward-bias dark current with increasing spacer layer thickness is also observed. In examining eq 1, this could imply a secondary cause for the variation of V_{OC} with spacer layer thickness beyond E_{CT} (E_{eff} in eq 1), as changes in the dark current (and hence J_0 in eq 1) also impact V_{OC}.[41] The relative dominance of one term over the other can be probed directly by examining the temperature dependence of V_{OC}. If E_{CT} is responsible for the change in V_{OC} with spacer layer thickness, different values of V_{OC} should be obtained at low temperature for each thickness. If the variation

DOI: 10.1021/acsami.5b03656
ACS Appl. Mater. Interfaces 2015, 7, 18306−18311

instead comes from changes in J_0, values of V_{OC} for all spacer layer devices should converge at low temperature. Figure 5c shows the temperature dependence of V_{OC} measured from 82 K to room temperature for CuPc-C_{60} PHJ OPVs, with a linear fit to the data over the range of 150−300 K to extrapolate the value of V_{OC} at 0 K. The 95% confidence intervals for the extracted values of V_0 are [0.94, 0.99] and [1.00, 1.03] for OPVs with no spacer layer and with a 3 nm-thick spacer layer, respectively. Thus, we conclude that the values of V_{OC} for devices constructed using various spacer layer thicknesses do not converge to the same value at low temperature, supporting a model where E_{CT} is increased with the insertion of a spacer layer, leading to the observed dependence of V_{OC} on spacer layer.

CONCLUSIONS

We have demonstrated a direct correlation between the charge-transfer state energy (E_{CT}) as extracted from electroluminescence and the theoretical maximum achievable V_{OC} in OPVs. This is in contrast to much previous work where only a partial correlation is made between E_{DA} and V_{OC}. The discrepancy between E_{CT} and E_{DA} is attributed to the binding energy of the CT state formed at the electron donor−acceptor interface. Here, the CT state binding energy is successfully modeled as a Coulombic electron−hole attraction. A wide energy gap spacer layer is used to effectively tune the size of the CT state and also the resulting V_{OC}.

AUTHOR INFORMATION

Corresponding Author

*(R.J.H.) E-mail: rholmes@umn.edu.

Notes

The authors declare no competing financial interest.

ACKNOWLEDGMENTS

This work was supported by the National Science Foundation (NSF) MRSEC Program under Award Number DMR-0819885 and through the NSF PREM Program under Award Number DMR-0934157. Support was also received from the University of Minnesota Initiative for Renewable Energy and the Environment. Y.Z. would also like to acknowledge support through a University of Minnesota Doctoral Dissertation Fellowship. The authors thank Dr. James Holst at Sigma-Aldrich Corporation for synthesizing DPDCPB and DTDCPB.

REFERENCES

(1) Tang, C. W. 2-Layer Organic Photovoltaic Cell. *Appl. Phys. Lett.* **1986**, *48*, 183−185.

(2) Peumans, P.; Yakimov, A.; Forrest, S. R. Small Molecular Weight Organic Thin-Film Photodetectors and Solar Cells. *J. Appl. Phys.* **2003**, *93*, 3693−3723.

(3) Zhang, M.; Irfan; Ding, H.; Gao, Y.; Tang, C. W. Organic Schottky Barrier Photovoltaic Cells Based on Moo_x/C_{60}. *Appl. Phys. Lett.* **2010**, *96*, 183301.

(4) Lo, M. F.; Ng, T. W.; Liu, T. Z.; Roy, V. A. L.; Lai, S. L.; Fung, M. K.; Lee, C. S.; Lee, S. T. Limits of Open Circuit Voltage in Organic Photovoltaic Devices. *Appl. Phys. Lett.* **2010**, *96*, 113303.

(5) Yang, B.; Guo, F.; Yuan, Y.; Xiao, Z.; Lu, Y.; Dong, Q.; Huang, J. Solution-Processed Fullerene-Based Organic Schottky Junction Devices for Large-Open-Circuit-Voltage Organic Solar Cells. *Adv. Mater.* **2013**, *25*, 572−577.

(6) Zou, Y.; Holmes, R. J. Influence of a Moox Interlayer on the Open-Circuit Voltage in Organic Photovoltaic Cells. *Appl. Phys. Lett.* **2013**, *103*, 053302.

(7) Zou, Y.; Holmes, R. J. The Role of Exciton Ionization Processes in Bulk Heterojunction Organic Photovoltaic Cells. *J. Mater. Chem. A* **2015**, *5*, 1500019.

(8) Park, S. H.; Roy, A.; Beaupre, S.; Cho, S.; Coates, N.; Moon, J. S.; Moses, D.; Leclerc, M.; Lee, K.; Heeger, A. J. Bulk Heterojunction Solar Cells with Internal Quantum Efficiency Approaching 100%. *Nat. Photonics* **2009**, *3*, 297−302.

(9) Di Nuzzo, D.; Wetzelaer, G.-J. A. H.; Bouwer, R. K. M.; Gevaerts, V. S.; Meskers, S. C. J.; Hummelen, J. C.; Blom, P. W. M.; Janssen, R. A. J. Simultaneous Open-Circuit Voltage Enhancement and Short-Circuit Current Loss in Polymer: Fullerene Solar Cells Correlated by Reduced Quantum Efficiency for Photoinduced Electron Transfer. *Adv. Energy. Mater.* **2013**, *3*, 85−94.

(10) Dimitrov, S. D.; Huang, Z.; Deledalle, F.; Nielsen, C. B.; Schroeder, B. C.; Ashraf, R. S.; Shoaee, S.; McCulloch, I.; Durrant, J. R. Towards Optimisation of Photocurrent from Fullerene Excitons in Organic Solar Cells. *Energy Environ. Sci.* **2014**, *7*, 1037−1043.

(11) Vandewal, K.; Widmer, J.; Heumueller, T.; Brabec, C. J.; McGehee, M. D.; Leo, K.; Riede, M.; Salleo, A. Increased Open-Circuit Voltage of Organic Solar Cells by Reduced Donor-Acceptor Interface Area. *Adv. Mater.* **2014**, *26*, 3839−3843.

(12) Chen, K. S.; Yip, H. L.; Salinas, J. F.; Xu, Y. X.; Chueh, C. C.; Jen, A. K. Y. Strong Photocurrent Enhancements in Highly Efficient Flexible Organic Solar Cells by Adopting a Microcavity Configuration. *Adv. Mater.* **2014**, *26*, 3349−3354.

(13) Rand, B.; Burk, D.; Forrest, S. Offset Energies at Organic Semiconductor Heterojunctions and Their Influence on the Open-Circuit Voltage of Thin-Film Solar Cells. *Phys. Rev. B: Condens. Matter Mater. Phys.* **2007**, *75*, 115327.

(14) Vandewal, K.; Tvingstedt, K.; Gadisa, A.; Inganas, O.; Manca, J. V. On the Origin of the Open-Circuit Voltage of Polymer-Fullerene Solar Cells. *Nat. Mater.* **2009**, *8*, 904−909.

(15) Vandewal, K.; Tvingstedt, K.; Gadisa, A.; Inganäs, O.; Manca, J. V. Relating the Open-Circuit Voltage to Interface Molecular Properties of Donor:Acceptor Bulk Heterojunction Solar Cells. *Phys. Rev. B: Condens. Matter Mater. Phys.* **2010**, *81*, 125204.

(16) Chen, S.; Tsang, S. W.; Lai, T. H.; Reynolds, J. R.; So, F. Dielectric Effect on the Photovoltage Loss in Organic Photovoltaic Cells. *Adv. Mater.* **2014**, *26*, 6125−6131.

(17) Gruber, M.; Wagner, J.; Klein, K.; Hörmann, U.; Opitz, A.; Stutzmann, M.; Brütting, W. Thermodynamic Efficiency Limit of Molecular Donor-Acceptor Solar Cells and Its Application to Diindenoperylene/C60-Based Planar Heterojunction Devices. *Adv. Energy. Mater.* **2012**, *2*, 1100−1108.

(18) Vandewal, K.; Tvingstedt, K.; Manca, J. V.; Inganas, O. Charge-Transfer States and Upper Limit of the Open-Circuit Voltage in Polymer:Fullerene Organic Solar Cells. *IEEE J. Sel. Top. Quantum Electron.* **2010**, *16*, 1676−1684.

(19) Hörmann, U.; Kraus, J.; Gruber, M.; Schuhmair, C.; Linderl, T.; Grob, S.; Kapfinger, S.; Klein, K.; Stutzman, M.; Krenner, H. J.; Brütting, W. Quantification of Energy Losses in Organic Solar Cells from Temperature-Dependent Device Characteristics. *Phys. Rev. B: Condens. Matter Mater. Phys.* **2013**, *88*, 235307.

(20) Hörmann, U.; Lorch, C.; Hinderhofer, A.; Gerlach, A.; Gruber, M.; Kraus, J.; Sykora, B.; Grob, S.; Linderl, T.; Wilke, A.; Opitz, A.; Hansson, R.; Anselmo, A. S.; Ozawa, Y.; Nakayama, Y.; Ishii, H.; Koch, N.; Moons, E.; Schreiber, F.; Brütting, W. Voc from a Morphology Point of View: The Influence of Molecular Orientation on the Open Circuit Voltage of Organic Planar Heterojunction Solar Cells. *J. Phys. Chem. C* **2014**, *118*, 26462−26470.

(21) Vandewal, K.; Albrecht, S.; Hoke, E. T.; Graham, K. R.; Widmer, J.; Douglas, J. D.; Schubert, M.; Mateker, W. R.; Bloking, J. T.; Burkhard, G. F.; Sellinger, A.; Fréchet, J. M. J.; Amassian, A.; Riede, M. K.; McGehee, M. D.; Neher, D.; Salleo, A. Efficient Charge Generation by Relaxed Charge-Transfer States at Organic Interfaces. *Nat. Mater.* **2014**, *13*, 63−68.

(22) Gommans, H.; Verreet, B.; Rand, B. P.; Muller, R.; Poortmans, J.; Heremans, P.; Genoe, J. On the Role of Bathocuproine in Organic Photovoltaic Cells. *Adv. Funct. Mater.* **2008**, *18*, 3686−3691.

DOI: 10.1021/acsami.5b03656
ACS Appl. Mater. Interfaces 2015, 7, 18306−18311

(23) Zou, Y.; Holst, J.; Zhang, Y.; Holmes, R. J. 7.9% Efficient Vapor-Deposited Organic Photovoltaic Cells Based on a Simple Bulk Heterojunction. *J. Mater. Chem. A* **2014**, *2*, 12397−12402.
(24) Chen, Y. H.; Lin, L. Y.; Lu, C. W.; Lin, F.; Huang, Z. Y.; Lin, H. W.; Wang, P. H.; Liu, Y. H.; Wong, K. T.; Wen, J.; Miller, D. J.; Darling, S. B. Vacuum-Deposited Small-Molecule Organic Solar Cells with High Power Conversion Efficiencies by Judicious Molecular Design and Device Optimization. *J. Am. Chem. Soc.* **2012**, *134*, 13616−13623.
(25) Barker, A. J.; Chen, K.; Hodgkiss, J. M. Distance Distributions of Photogenerated Charge Pairs in Organic Photovoltaic Cells. *J. Am. Chem. Soc.* **2014**, *136*, 12018−12026.
(26) Widmer, J.; Tietze, M.; Leo, K.; Riede, M. Open-Circuit Voltage and Effective Gap of Organic Solar Cells. *Adv. Funct. Mater.* **2013**, *23*, 5814−5821.
(27) Koster, L. J. A.; Mihailetchi, V. D.; Ramaker, R.; Blom, P. W. M. Light Intensity Dependence of Open-Circuit Voltage of Polymer:-Fullerene Solar Cells. *Appl. Phys. Lett.* **2005**, *86*, 123509.
(28) Cowan, S. R.; Roy, A.; Heeger, A. J. Recombination in Polymer-Fullerene Bulk Heterojunction Solar Cells. *Phys. Rev. B: Condens. Matter Mater. Phys.* **2010**, *82*, 245207.
(29) Pandey, R.; Holmes, R. J. Graded Donor-Acceptor Heterojunctions for Efficient Organic Photovoltaic Cells. *Adv. Mater.* **2010**, *22*, 5301−5305.
(30) Jeong, W. I.; Lee, Y. E.; Shim, H. S.; Kim, T. M.; Kim, S. Y.; Kim, J. J. Photoconductivity of C60 as an Origin of Bias-Dependent Photocurrent in Organic Photovoltaics. *Adv. Funct. Mater.* **2012**, *22*, 3089−3094.
(31) Cho, S. W.; Piper, L. F. J.; DeMasi, A.; Preston, A. R. H.; Smith, K. E.; Chauhan, K. V.; Sullivan, P.; Hatton, R. A.; Jones, T. S. Electronic Structure of C60/Phthalocyanine/Ito Interfaces Studied Using Soft X-Ray Spectroscopies. *J. Phys. Chem. C* **2010**, *114*, 1928−1933.
(32) Djurovich, P. I.; Mayo, E. I.; Forrest, S. R.; Thompson, M. E. Measurement of the Lowest Unoccupied Molecular Orbital Energies of Molecular Organic Semiconductors. *Org. Electron.* **2009**, *10*, 515−520.
(33) Kim, H.; Kim, J. Y.; Park, S. H.; Lee, K.; Jin, Y.; Kim, J.; Suh, H. Electroluminescence in Polymer-Fullerene Photovoltaic Cells. *Appl. Phys. Lett.* **2005**, *86*, 183502.
(34) Westenhoff, S.; Howard, I. A.; Hodgkiss, J. M.; Kirov, K. R.; Bronstein, H. A.; Williams, C. K.; Greenham, N. C.; Friend, R. H. Charge Recombination in Organic Photovoltaic Devices with High Open-Circuit Voltages. *J. Am. Chem. Soc.* **2008**, *130*, 13653−13658.
(35) Tvingstedt, K.; Vandewal, K.; Gadisa, A.; Zhang, F.; Manca, J.; Inganäs, O. Electroluminescence from Charge Transfer States in Polymer Solar Cells. *J. Am. Chem. Soc.* **2009**, *131*, 11819−11824.
(36) Faist, M. A.; Kirchartz, T.; Gong, W.; Ashraf, R. S.; McCulloch, I.; de Mello, J. C.; Ekins-Daukes, N. J.; Bradley, D. D. C.; Nelson, J. Competition between the Charge Transfer State and the Singlet States of Donor or Acceptor Limiting the Efficiency in Polymer:Fullerene Solar Cells. *J. Am. Chem. Soc.* **2012**, *134*, 685−692.
(37) Deibel, C.; Strobel, T.; Dyakonov, V. Role of the Charge Transfer State in Organic Donor−Acceptor Solar Cells. *Adv. Mater.* **2010**, *22*, 4097−4111.
(38) Campbell, I. H.; Crone, B. K. Improving an Organic Photodiode by Incorporating a Tunnel Barrier between the Donor and Acceptor Layers. *Appl. Phys. Lett.* **2012**, *101*, 023301.
(39) Liu, F.; Crone, B. K.; Paul Ruden, P.; Smith, D. L. Control of Interface Microscopic Processes in Organic Bilayer Structures and Their Effect on Photovoltaic Device Performance. *J. Appl. Phys.* **2013**, *113*, 044516.
(40) Fukagawa, H.; Watanabe, K.; Tsuzuki, T.; Tokito, S. Highly Efficient, Deep-Blue Phosphorescent Organic Light Emitting Diodes with a Double-Emitting Layer Structure. *Appl. Phys. Lett.* **2008**, *93*, 133312.
(41) Perez, M. D.; Borek, C.; Forrest, S. R.; Thompson, M. E. Molecular and Morphological Influences on the Open Circuit Voltages of Organic Photovoltaic Devices. *J. Am. Chem. Soc.* **2009**, *131*, 9281−9286.
(42) Cho, S. W.; Piper, L. F. J.; DeMasi, A.; Preston, A. R. H.; Smith, K. E.; Chauhan, K. V.; Hatton, R. A.; Jones, T. S. Soft X-Ray Spectroscopy of C60/Copper Phthalocyanine/Moo3 Interfaces: Role of Reduced Moo3 on Energetic Band Alignment and Improved Performance. *J. Phys. Chem. C* **2010**, *114*, 18252−18257.

DOI: 10.1021/acsami.5b03656
ACS Appl. Mater. Interfaces 2015, 7, 18306−18311